

A sensitive method for examining whole-cell biochemical composition in single cells of filamentous fungi using synchrotron FTIR spectromicroscopy

Konstantin Jilkine^a, Kathleen M. Gough^a, Robert Julian^b, Susan G.W. Kaminskyj^{c,*}

^a Department of Chemistry, University of Manitoba, Winnipeg, MB, Canada R3T 2N2

^b Synchrotron Radiation Centre (SRC), University of Wisconsin at Madison, Stoughton, WI 53589, USA

^c Department of Biology, University of Saskatchewan, Saskatoon, SK, Canada S7N 5E2

Received 9 July 2007; received in revised form 7 October 2007; accepted 19 October 2007

Available online 23 November 2007

Abstract

Cell function is related to cell composition. The asexual state of filamentous fungi (molds and mildews) has two main life cycle stages: vegetative hyphae for substrate colonization and nutrient acquisition, and asexual spores for survival and dispersal. Hyphal composition changes over a few tens of microns during growth and maturation; spores are different from hyphae. Most biochemical analyses are restricted to studying a few components at high spatial resolution (*e.g.* histochemistry) or many compounds at low spatial resolution (*e.g.* GC–MS). Synchrotron FTIR spectromicroscopy can be used to study fungal cell biology by fingerprinting varieties of carbohydrates, proteins, and lipids at about 6 μm spatial resolution. FTIR can distinguish fungal species and changes during hyphal growth, and reveals that even fungi grown under optimal *vs* mildly stressed conditions exhibit dramatic biochemical changes without obvious morphological effects. Here we compare hypha and spore composition of two fungi, *Neurospora* and *Rhizopus*. There are clear biochemical changes when *Neurospora* hyphae commit to spore development, during spore maturation and following germination, many of which are consistent with results from molecular genetics, but have not been shown before at high spatial resolution. *Rhizopus* spores develop within a fluid-containing sporangium that becomes dry at maturity. *Rhizopus* spores had similar protein content and significantly more carbohydrate than the sporangial fluid, both of which are novel findings.

© 2007 Elsevier Inc. All rights reserved.

Keywords: Filamentous fungi; *Neurospora*; *Rhizopus*; Spores; Synchrotron FTIR spectromicroscopy

1. Introduction

Fungi play key roles in the environment, having major positive impacts on terrestrial plant survival through mycorrhizal symbioses, being essential for herbivore nutrition through assisting cellulose digestion, and being critical to recycling dead plant materials. Some species are used in ancient and modern biotechnology, and as model experimental systems. Other species, both as plant and human pathogens, are established or emerging threats. Fungi inter-

act with their surroundings through their cell walls and by means of the compounds they secrete (particularly for nutrient acquisition) or store (particularly for defense or reproduction). The fungal wall supports and protects the cytoplasm, maintains cell shape, and permits force generation required for substrate penetration [1–3].

Cell function is intrinsically related to cell composition. The asexual state of filamentous fungi (molds and mildews) has two main life cycle stages: vegetative hyphae for substrate colonization and nutrient acquisition [1,4] and spores for survival and dispersal (*e.g.* [5]). The sexual state is transient at best. The vegetative life cycle of a typical mold begins with spore germination followed by development

* Corresponding author. Tel.: +1 306 966 4422; fax: +1 306 966 4461.
E-mail address: Susan.Kaminskyj@usask.ca (S.G.W. Kaminskyj).

of a mycelium composed of branched tubular hyphae that invade a nutrient substrate. During hyphal growth, cell extension is localized to the tip. The wall matures by about 10 μm from the extending apex [6,7] depending on the species and growth rate, whereas cytoplasm composition continues to change over tens of microns as hyphae invade a substrate, acquire nutrients, and metabolize them. At the hyphal tip the cytoplasm is largely composed of exocytic vesicles and associated cytoskeletal machinery, which intergrades basally into cytoplasm containing biosynthetic organelles [8,9]. In molds, asexual spore development occurs preferentially in mature colony regions. Hyphal wall composition differs between major taxonomic groups [10] as well as there being changes along the length of the hypha that are associated with maturation. Spore wall structure [11] and metabolite profile [12,13] show major changes during development and again during germination. Sporulation is genetically programmed [5] but is influenced by environmental stress, including resource limitation.

The composition of fungal walls and cytoplasm varies dramatically over a few microns during hyphal germination and growth, and during spore development. The number and types of component that can be studied simultaneously is inversely related to the spatial resolution of the analysis. The identity of hundreds of components can be resolved in bulk samples using GC–MS; the distribution and behaviour of specific components within particular cells can be resolved using fluorescent protein tagging or with histochemistry. Single-cell FTIR spectromicroscopy can span this technique-related gulf, generating subcellular biochemical fingerprints of carbohydrates, proteins and lipids [14] with spatial resolution at the diffraction limit of the infrared spectrum (as low as 3 μm at the shorter wavelengths).

FTIR analysis of fungal cells is challenging because much of the relevant information on cell walls and energy sources resides in the carbohydrate composition. However, the most distinctive carbohydrate signatures appear at the longer infrared wavelengths where the diffraction limit is realistically on the order of 5–10 μm . In addition, the dimension of the spores and conidiophores is on the order of the wavelength of the light, so the spectra are prone to scattering artifacts. Finally, the amount of material is low, so the signal from individual spores or from hyphal tips is weak. With a synchrotron source to offset these issues, FTIR can probe subtle and cell type-specific biochemical differences in fungal systems.

Our previous work [14] used synchrotron FTIR to characterize the biochemical components of individual *Aspergillus nidulans*, *Neurospora*, and *Rhizopus* hyphae. For each species, there were dramatic biochemical differences between tip and subapical (*i.e.* younger and older) regions, and overall there were substantial differences between *Aspergillus* and *Neurospora* (Ascomycetes) and *Rhizopus* (Zygomycetes). In addition, there were clear differences in hyphal composition for cells grown at optimal compared to stressed (pH, temperature) conditions. Here,

we used synchrotron FTIR spectromicroscopy to examine spores of *Neurospora* and *Rhizopus*.

2. Materials and methods

2.1. Fungi

MirrIR low-e microscope slides (Kevley Technologies, www.tientasciences.com) or gold-coated silicon wafers (in-house, U. Manitoba) were used as substrates for FTIR. Wildtype strains of *Neurospora* and *Rhizopus*, isolated from nature, were grown from 3 mm \times 3 mm \times 8 mm pieces of Difco potato dextrose agar (www.vwrcanada.com) adjusted to pH 5.0, 6.5 or 8.5, inoculated with freshly harvested spores. These were placed on the imaging substrate and incubated inverted (supported by glass tubing) in moist chambers for 8–24 h at 28 °C. During incubation hyphae grew out from the agar across the imaging substrate. Once hyphae had grown sufficiently, samples were frozen on a metal slab at –80 °C for 30 min, then lyophilized (Freezone 6; www.labconco.com) to dryness. Cells were imaged prior to FTIR spectrum collection using a Nikon Alphaphot-2 YS2-H microscope and 10x N.A. 0.25 objective, or a 40x N.A. 0.65 objective, using reflected light. Images were collected with a 5.1 megapixel Nikon Coolpix 5400 CCD.

Due to their large size, upright orientation, and rounded morphology, *Rhizopus* sporangia are difficult to analyze using single-cell FTIR. To study *Rhizopus* spores, samples were warmed to 0 °C for 1–2 s just prior to lyophilization to collapse the sporangiophores onto the substrate. Sporangia induced to collapse provided excellent subjects for spectroscopy.

2.2. FTIR spectromicroscopy

All spectra were recorded in reflectance mode using synchrotron radiation on a Nicolet Magna 500 equipped with continuum microscope (SRC) or with a standard globar lamp on a Bruker Tensor FTIR with Hyperion confocal microscope/mapping stage (U. Manitoba). Either the Nicolet Omnic software or the Bruker Opus software was used for data acquisition and analyses. Pixel size for the synchrotron studies was generally 6–8 μm ; for the bench instrument this was increased to at least 25 μm \times 25 μm . For synchrotron source spectra, typically 256–1024 interferograms were collected for each pixel, co-added and ratioed to a similar background scan recorded at a blank region of the slide. For the bench instrument, up to 4096 scans were co-added for both background and sample. Individual spectra and maps (line and area maps) were saved in log(1/R) format, 4 cm^{-1} resolution, encompassing the mid-IR region from 4000 to 800 cm^{-1} , with no zero-filling level. No further processing of data (smoothing, Fourier self deconvolution, etc) was employed, to avoid the introduction of artifacts. Peak assignments were the same as for [14]. The spectra presented are typical of at least

six replicate hyphae per strain and growth condition. Spectra are vertically offset for visual clarity.

3. Results

3.1. *Neurospora* hyphae grown on media with different pH

Neurospora grows well over a broad pH range. We chose pH 6.5 to approximate optimum pH, and to be consistent with *A. nidulans* complete medium [15] used previously [14]. Colony growth on pH 5.0 medium and pH 8.5 medium were qualitatively similar to pH 6.5 as far as hyphal extension; sporulation was somewhat more abundant at pH 8.5.

Fig. 1 shows spectra of apparently healthy *Neurospora* hyphae grown at (a) pH 5.0, (b) pH 6.5, and (c) pH 8.5. Hyphal composition varies with distance from the tip [14], so spectra were collected at the distances (in μm)

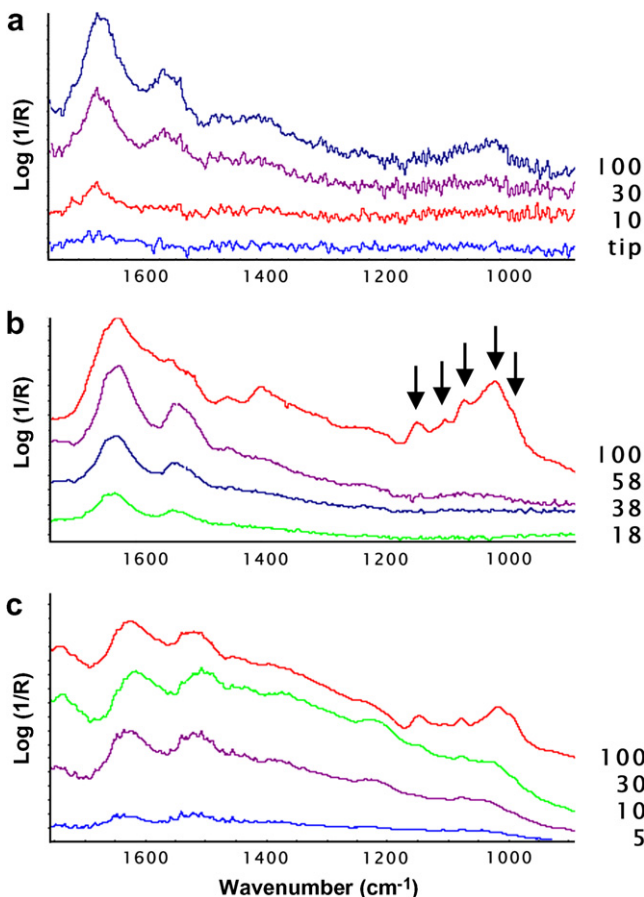


Fig. 1. Vegetative hyphae of *Neurospora* grown at: (a) pH 5.0, (b) pH 6.5, and (c) pH 8.5. Spectra are shown in $\log(1/R)$ format, the equivalent of absorbance for reflectance spectra, presented on the same scale within each group, and offset vertically for clarity. Absorbance (vertical axis) displays 0.06, 0.30, and 0.40 units for A, B, and C, respectively. Horizontal axis displays wavenumbers (inverse wavelength) between 1820 and 880 cm^{-1} . For hyphae grown at pH 5, each spectrum is the sum of 1024 scans, whereas for cells grown at pH 6.5 and 8.5, each spectrum is the sum of 256 scans. All spectra are corrected for atmospheric water. The arrows in (b) indicate peak positions of 1148, 1110, 1078, 1030, and 995 cm^{-1} , which are typical of glycogen-like compounds.

behind the tip as indicated. At each growth pH, hyphae had relatively prominent protein compared to carbohydrate content. Hyphal tips had relatively low biomass, so there was low signal across the spectrum despite using synchrotron light and summing 1024 (a) or 256 (b,c) scans per pixel. Despite the four-fold larger number of scans per pixel used for the hypha grown at pH 5.0, noise remained relatively high indicating that this cell had extremely low biomass. Signal strength was considerably better for hyphae grown at pH 6.5 and 8.5: these spectra were summed from fewer scans, had higher $\log(1/R)$, and the spectra had lower noise.

The chemical content at the growing tips of vegetative hyphae was very low, as evidenced by the very low intensity of the protein amide I and II bands centered about 1650 and 1530 cm^{-1} in all three examples (Fig. 1 a, b, and c bottom spectrum in each group). Protein content increased subapically, that is, as the hypha matured. The amide I and II bands are less well-resolved in the mature hyphae. Other biochemical components with amide-like linkages (including chitin and chitosan) are also present in fungi which may be contributing to this region [16].

The 1150–900 cm^{-1} region encompasses a carbohydrate fingerprint region that includes β -1,3-glucans, galactomannans, β -1,4-glucans [14] and trehalose [17]. The signal in this region was much stronger for hyphae grown at pH 6.5 (Fig. 1b) suggesting that this pH is indeed near optimal. We had previously shown that growth at elevated pH was associated with weaker walls [14]. Less robust growth at pH 5.0, particularly shown by reduced carbohydrate content, was not anticipated since fungi secrete organic acids during growth for nutrient acquisition, and so tend to acidify their media over time. However, particularly for hyphae grown at pH 5.0 the total biomass was substantially reduced compared to growth at pH 6.5: the maximum value on the pH 5.0 $\log(1/R)$ scale was 0.08, compared to 0.4

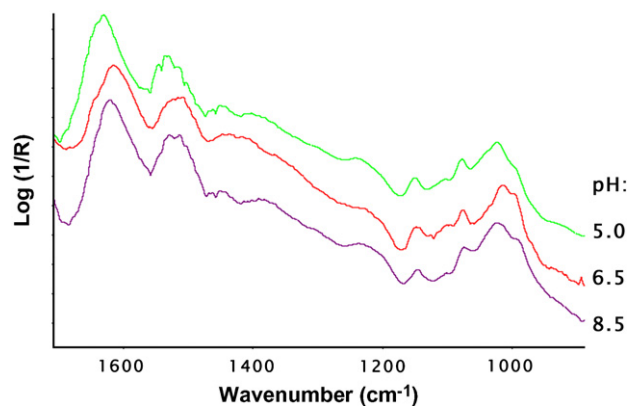


Fig. 2. Mature spores grown at pH 5.0 (top), 6.5 (middle), and 8.5 (bottom). The spectrum at pH 5.0 was recorded from a small cluster of mature spores, with a Bruker Hyperion, global source, aperture of 35 $\mu\text{m} \times 40 \mu\text{m}$, co-addition of 4096 scans, ratioed to a similar background. Spectra for pH 6.5 and 8.5 were recorded from mature spores, with a continuum microscope and synchrotron source (SRC), aperture of 8 $\mu\text{m} \times 8 \mu\text{m}$, co-addition of 256 scans ratioed to a similar background.

for pH 6.5 and 0.4 for pH 8.5. At both pH 5.0 and 8.5 the protein signal (amide I and II) was relatively higher than for the carbohydrate region, suggesting that *Neurospora* compensates for weaker walls by increasing the strength of its protein cytoskeleton.

3.2. Mature *Neurospora* spores

Fig. 2 shows spectra collected from mature *Neurospora* spores grown at pH 5.0, 6.5, 8.5. Regardless of the pH of the growth medium, these mature spores had a consistent spectral signature, with strong protein and sugar bands. The spectra at pH 6.5 and 8.5 both exhibited a relatively

strong peak at about 990 cm^{-1} , possibly due to the presence of trehalose [17].

3.3. *Neurospora* spore development

Mature spores (Figs. 2 and 3a) had a well-developed FTIR spectrum indicating a high concentration of protein and sugar, as well as nucleic acids, as expected for a biochemically rich material. In contrast, a hypha that had committed to sporulation but not yet formed mature spores had little material at the growing tip (Fig. 3b, spectrum 1), as was typically observed. This could also indicate an immature spore that was forming at the tip. There was a

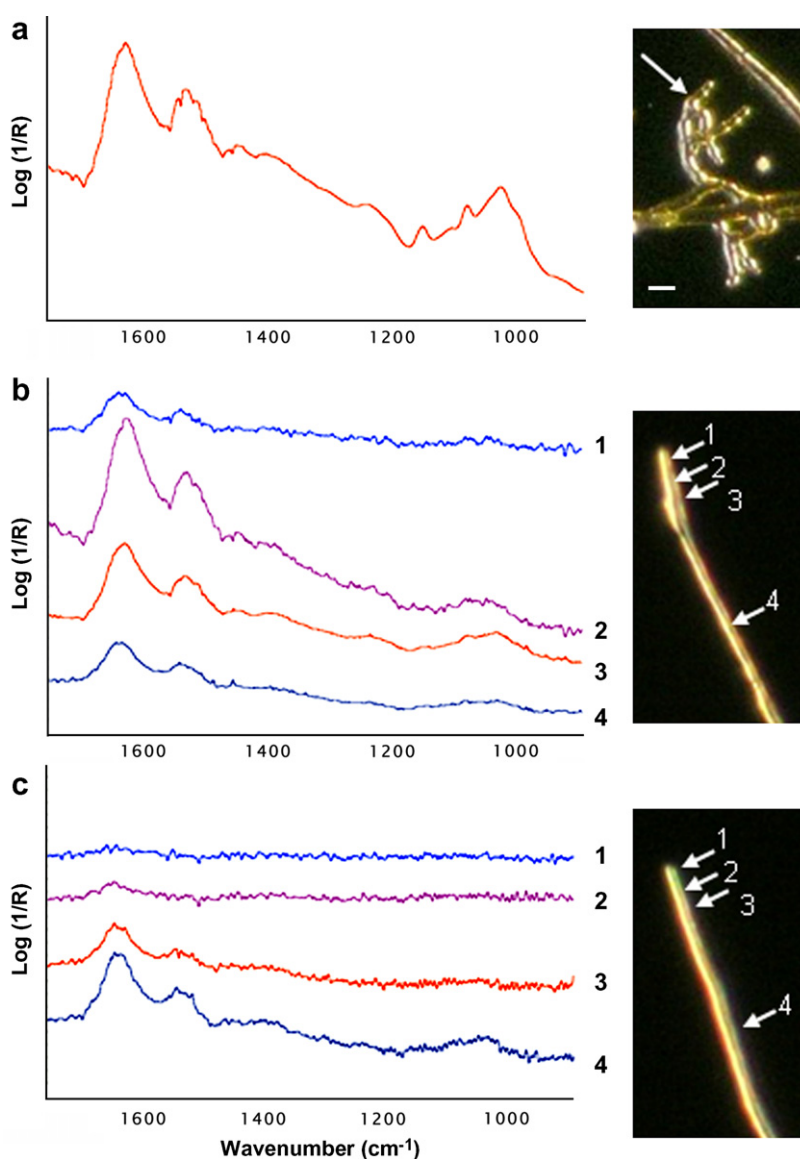


Fig. 3. Spore development in *Neurospora* grown at pH 5.0. (a) Mature spores, (b) a hypha with developing spores at its apex, and (c) a vegetative hypha. The spectrum in (a) was collected as described in Fig. 2, and all spectra were collected at the positions indicated on the images. Images were acquired by CCD at U. Manitoba prior to FTIR spectrum collection at SRC. The spectra in b and c are co-added from 256 scans per pixel, pixel size $8\ \mu\text{m} \times 8\ \mu\text{m}$, using data collected at SRC. All spectra have been corrected for atmospheric water, and all are displayed at the same vertical $\log(1/R)$ axis scale of 0.01–0.34 units; within a group, they are vertically offset for clarity. There is no change in the absolute intensity of spectral bands, so that they may be compared directly. Bar = $10\ \mu\text{m}$, for all parts.

significant increase in the amount of protein just behind this first site (Fig. 3b, spectrum 2), showing that the enzymes and potentially the organelles required for spore development were present in abundance. At 30 μm behind the tip (Fig. 3b, spectrum 3), the distinctive sugar signature of a spore was becoming evident, although the quantity of sugars relative to protein is less than that observed in mature spores (Fig. 2). Finally, at 100 μm behind the tip (Fig. 3b, spectrum 4), the hypha exhibited the normal profile of a vegetative hypha. In marked contrast, the spectra from the same relative locations in the vegetative hypha (Fig. 3c, spectra 1–4) showed only low biochemical content, initially some protein and eventually some maturing cell wall.

3.4. *Neurospora* spore germination

Fig. 4 shows an isolated spore from a colony grown at pH 8.5, which was germinating on the FTIR substrate. All of the metabolites for early stages of germination and growth are contained in the spore, which only needs water and the presence of a carbon metabolite to initiate germination [12]. The arrows on the image in Fig. 4 indicate where the spectra were collected; the spectra are presented in the same spatial order as the arrows. The germinated spore (Fig. 4a, arrow 1) has relatively high lipid (Fig. 4b, spectrum 1), carbohydrate and protein (Fig. 4c, top spectrum) reserves, even after the germ tube was more than 100 μm long. Lower levels of these reserves are present in the germ tube cytoplasm adjacent to the spore (Fig. 4a, arrows 2 and 3; Fig. 4b, spectra 2 and 3; Fig. 4c, second and third spectra from the top). Notably, the lipid profile in the cytoplasm adjacent to the germinated spore showed qualitative changes (Fig. 4b, spectra 2 and 3) with respect to the spore, and the putative trehalose peak had disappeared (Fig. 4c, second and third spectra from the top). In regions of the germ tube relatively distant from the spore (bottom five spectra), the carbohydrate content was low, and the spectra resembled established vegetative hyphae.

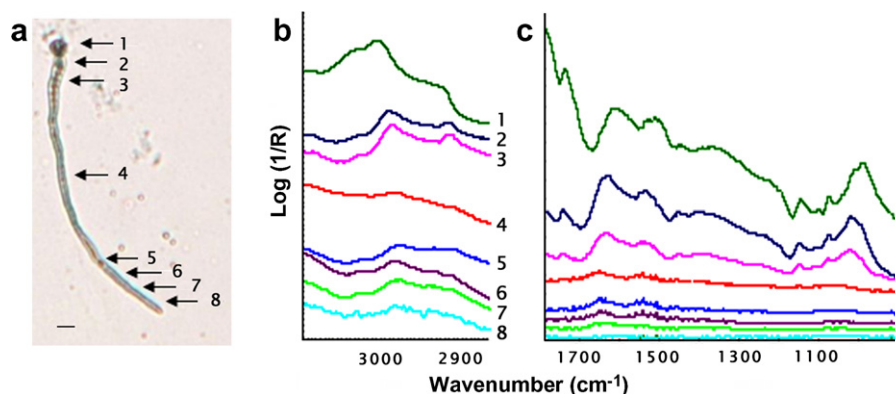


Fig. 4. *Neurospora* spore germination, producing a short germling, shown in (a). This sample was grown at pH 8.5. For each of (b) the CH₂ region, and (c) the amide and sugar region, the vertical order of spectra corresponds to the order of arrows shown on the image. Bar = 10 μm . Even several hours after germination, the germinated spore contains substantial quantities of lipid, protein, and carbohydrate (spectrum 1). In contrast, the growing tip of the germling (spectrum 8) has relatively low biomass content, and that mostly as lipid and protein.

3.5. *Rhizopus* sporangium

Fig. 5 shows a *Rhizopus* sporangium containing immature spores that had collapsed onto the imaging substrate and ruptured. The image (a) shows the dark sporangio-phore (sph) and rounded apical columella (c) that supported the developing sporangium, and the dried fluid (f) that was released upon rupture of the sporangium wall (spw). The maps and representative spectra show the relative content of lipid (c), protein (d), and carbohydrate (e) for the area boxed in red on the image. The edges of the box and points therein indicate the center of each pixel, so the map appears to be larger than the box. The columella has a strongly rounded profile that interferes with efficient acquisition of FTIR spectral information particularly in the carbohydrate region, so its signal strength in that region was attenuated.

4. Discussion

The major value of synchrotron FTIR spectromicroscopy over many other bioanalytical methods is its ability to distinguish between subtle changes in overall cell biochemical composition even in the absence of morphological differences. In addition, composition can be assessed at high spatial resolution, even within a single cell.

Our previous work showed that hyphae grown in media with slightly alkaline pH tended to be less sturdy than those grown at optimum pH [14]. Since fungi typically acidify their growth medium over time [1], we were surprised to find that *Neurospora* hyphae grown in pH 5 medium were less robust than in pH 8.5 medium. At each of these suboptimal pH levels, cell carbohydrate content was more affected than that of protein, suggesting that when wall synthesis is reduced, *Neurospora* hyphae may reinforce their hyphae by increasing their internal actin and microtubule protein cytoskeletons. Consistent with this, the *Neurospora* slime mutant, whose walls are severely depleted

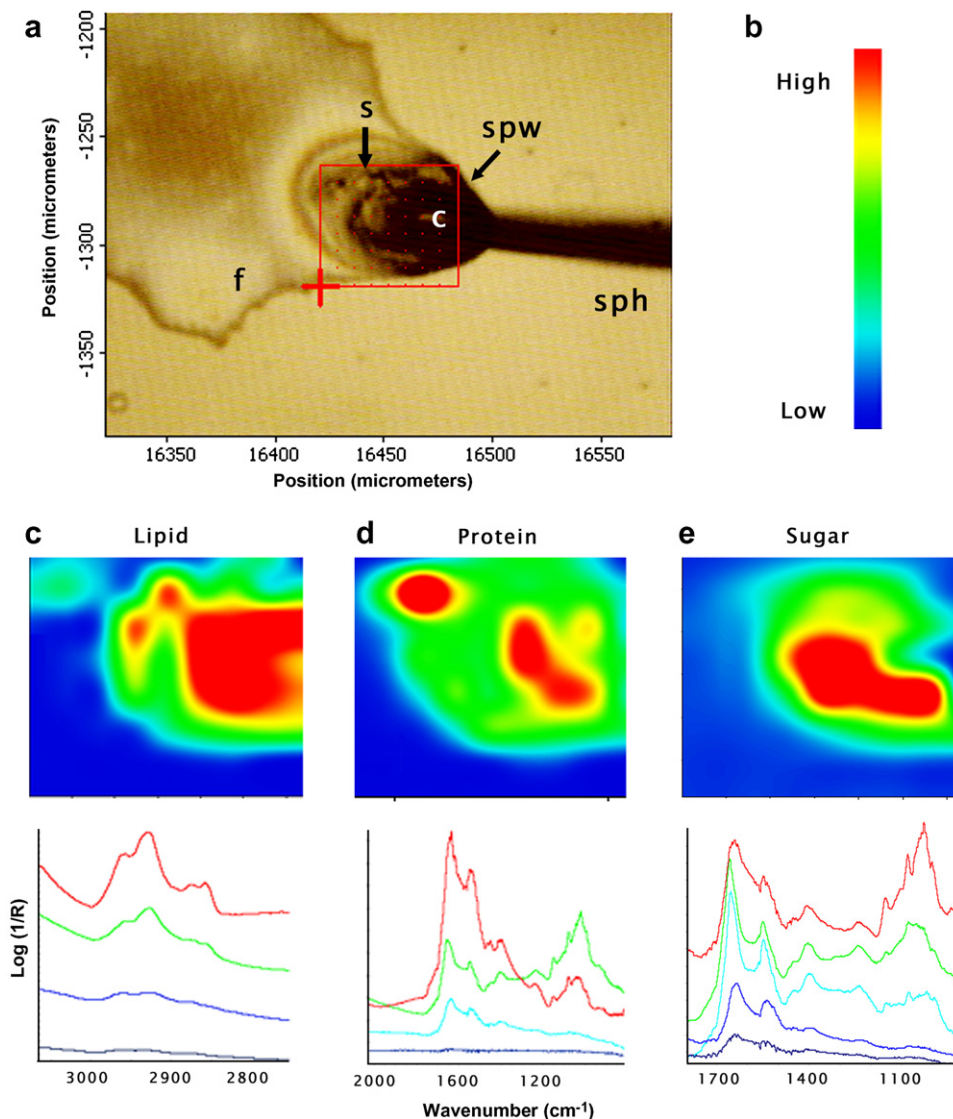


Fig. 5. Developing *Rhizopus* sporangium. This sporangiophore (sph) that supports the sporangium had collapsed onto the imaging substrate, rupturing the sporangium wall (spw) releasing fluids (f) that had bathed the developing spores, shown in the CCD image (a). The columella (c) is a dense rounded structure within the sporangium. Several oval spores (s) are visible within the mapped area (red box). The edges of the box and the points therein indicate the centers of the pixels from which the spectra were collected. (b) The mapping colour scale. (c) Map and representative spectra for lipids: symmetric CH_2 stretch, the total area from $2864\text{--}2847\text{ cm}^{-1}$, using $2887\text{--}2833\text{ cm}^{-1}$ as a baseline. (d) Map and representative spectra for proteins: amide I, the total area under $1661\text{--}1624\text{ cm}^{-1}$, using $1754\text{--}831\text{ cm}^{-1}$ as a baseline. (e) Map and representative spectra for sugars: the total area under $1048\text{--}1013\text{ cm}^{-1}$, using $1167\text{--}951\text{ cm}^{-1}$ as a baseline.

for chitin, can nevertheless produce hypha-shaped extrusions, called pseudoplasmodia [18].

Neurospora colonies were grown in media at pH 5.0, 6.5, and 8.5, in order to study the effect of mild environmental stress on spores. Sporulation can be triggered by resource limitation or stress [5]. Asexual fungal spores are important for biotechnology and are the main infectious propagules in the environment, so better understanding of sporulation-related processes is essential. In general, pH 6.5 medium is near-optimal, although this depends in part on whether growth is quantified as colony linear expansion, wet or dry biomass accumulation, or spore production. Fungi secrete organic acids during growth that are involved in nutrient acquisition [1] typically reducing medium pH

over time, consistent with growth in medium with an alkaline pH appearing to be stressful [14]. Unlike the pronounced compositional changes seen between hyphae grown at different pH levels, the spores produced by these colonies had similar composition. It appears that *Neurospora* can preferentially translocate nutrients to its spores, perhaps even at the expense of the vegetative mycelium.

We restricted our FTIR analysis to morphologically normal hyphae, but found that these did not necessarily have uniform FTIR spectra. As in this study, experiments described in [14] examined large numbers of hyphae. For hyphae of a single species, grown under the same nutrient conditions, showing similar morphology and examined at comparable distances behind the hyphal tip, most differ-

ences related to intensity of bands. A few hyphae had dramatically reduced carbohydrate and protein content, resembling the spectra collected from hyphal tips. This is evidence of the sensitivity of synchrotron FTIR spectromicroscopy, may relate to heterogeneity between hyphae in a single colony. Where possible, we analyzed hyphae that provided good signal/noise. Hubbard and Kaminskyj [19] showed that in a population of 221 morphologically similar, untreated *A. nidulans* hyphae, 109 failed to grow during a 2–5 min observation period. This growth disparity [19] appears to correlate with the biochemical heterogeneity reported herein, and argues for large sample sizes and cautious interpretation.

The biochemical patterns seen during *Neurospora* spore development are consistent with preferential translocation of metabolites to sporulating structures. The metabolite content in a *Neurospora* hypha that has committed to sporulation (having a beaded appearance at the hyphal tip) showed a different pattern of protein and carbohydrate accumulation from vegetative hyphae. Similarly, the lipid, protein and sugar content of immature *Rhizopus* spores was considerably higher than previously seen for vegetative hyphae [14].

Trehalose is the most common fungal disaccharide and is usually found together with sugar alcohols and glycogen, but at higher concentrations [20]. Trehalose accumulation is correlated with asexual spore development, environmental stresses including growth at high temperature [13,20] and desiccation, which is necessary for dormancy of air dispersed spores. Trehalose mobilization is one of the main biochemical events in early spore germination [12,20,21]. In *Neurospora*, trehalose synthase *csg9* activity precedes by several hours that of sporulation-related genes like *csg2* [13,22], which encodes a hydrophobic protein associated with spore surfaces [11,22].

In conclusion, we have shown that synchrotron FTIR spectromicroscopy can provide spatially-resolved biochemical information on fungal spore development that complements information gleaned from molecular genetic investigations. We anticipate that this technique, in con-

junction with focal plane array detection and FTIR-compatible humidity cells for live cell visualization currently under development at SRC, will enable real-time biochemical imaging at better than 5 μm spatial resolution.

Acknowledgements

We are pleased to acknowledge NSERC Discovery Grant awards to K.M.G. and S.G.W.K., and an NSERC USRA to K.J. Research at the Synchrotron Radiation Centre is supported by NSF Award No. DMR-08442.

References

- [1] N.A.R. Gow, G.M. Gadd, in: *The Growing Fungus*, Chapman and Hall, London, 1995, p. 473.
- [2] S.G.W. Kaminskyj, I.B. Heath, *Mycologia* 88 (1996) 20–37.
- [3] N.P. Money, *Mycologist* 18 (2004) 71–76.
- [4] S. Bartnicki-Garcia, in: *Molecular Biology of Fungal Development*, Marcel Dekker, NY, 2002, pp. 29–58.
- [5] J.E. Hamer, G. Lau, *The Mycologist*, vol. 8, Springer-Verlag, Heidelberg, 2007, pp. 263–292.
- [6] G.M. Guest, M. Momany, *Mycologia* 92 (2000) 1047–1050.
- [7] H. Ma, L.A. Snook, S.G.W. Kaminskyj, T.E.S. Dahms, *Microbiology (Reading)* 151 (2005) 3679–3688.
- [8] S.N. Grove, C.E. Bracker, *J. Bacteriol.* 104 (1970) 989–1009.
- [9] R.J. Howard, *J. Cell Sci.* 48 (1981) 9–103.
- [10] S. Bartnicki-Garcia, *Ann. Rev. Microbiol.* 55 (1968) 87–108.
- [11] M.J. Kershaw, N.J. Talbot, *Fungal Genet. Biol.* 23 (1998) 18–33.
- [12] C. d'Enfert, *Fung. Genet. Biol.* 21 (1997) 163–172.
- [13] M.L. Shinohara, A. Correa, D. Bell-Pederson, J.C. Dunlap, J.J. Loros, *Euk. Cell* 1 (2002) 33–43.
- [14] A. Szeghalmi, S. Kaminskyj, K.M. Gough, *Anal. Bioanal. Chem.* 387 (2007) 1779–1789.
- [15] S.G.W. Kaminskyj, *Fungal Genet. Newsl.* 48 (2001) 25–31.
- [16] J.H. Sietsma, J.G.H. Wessels, *J. Gen. Microbiol.* 114 (1979) 99–108.
- [17] W.F. Wolkers, A.E. Oliver, F. Tablina, J.H. Crowe, *Carbohydr. Res.* 339 (2004) 1077–1085.
- [18] I.B. Heath, G. Steinberg, *Fungal Genet. Biol.* 28 (1999) 79–93.
- [19] M.A. Hubbard, S.G.W. Kaminskyj, *Mycol. Prog.* 6 (2007) 179–189.
- [20] J.M. Thevelein, *Microbiol. Rev.* 48 (1984) 42–59.
- [21] M.A. Singer, S. Lindquist, *Trends Biotech.* 16 (1998) 460–468.
- [22] D. Bell-Pederson, J.C. Dunlap, J.J. Loros, *Mol. Biol. Cell* 16 (1996) 513–521.